




## Original Research Article

# Effect of deposition potential on the structural and optical properties of electrodeposited antimony doped zinc telluride (Sb:ZnTe) thin films for optoelectronic applications

Victor Chukwuagozie Onuabuchi <sup>1\*</sup> , Asad Ullah <sup>2</sup>, Nkechi Josephine Opene <sup>3</sup>, Tai Yanlong <sup>4</sup>, Chukwuemeka Innocent Elekalachi <sup>5</sup>, Nonso Livinus Okoli <sup>6</sup>

<sup>1</sup> Department of Industrial Physics, Enugu State University of Science and Technology, Agbani, Enugu State, Nigeria

<sup>2</sup> Centre of Excellence in Solid State Physics, University of the Punjab, Lahore, Pakistan

<sup>3</sup> Department of Science Laboratory Technology, Delta State Polytechnic, Ogwashi – Uku, Delta State, Nigeria

<sup>4</sup> Shenzhen Institutes of Advanced Technology, CAS, Shenzhen, 518055, China

<sup>5</sup> Department of Industrial Physics, Chukwuemeka Odumegwu Ojukwu University Uli, Anambra State, Nigeria

<sup>6</sup> Department of Computer Science Education, Madonna University Nigeria, Okija Campus, Anambra State, Nigeria

### ARTICLE INFORMATION

Submitted: 2024-02-22

Revised: 2024-03-19

Accepted: 2024-04-05

Manuscript ID: JMNC-2402-1019

Checked for Plagiarism: **Yes**

Language Editor Checked: **Yes**

DOI: 10.48309/JMNC.2024.1.5

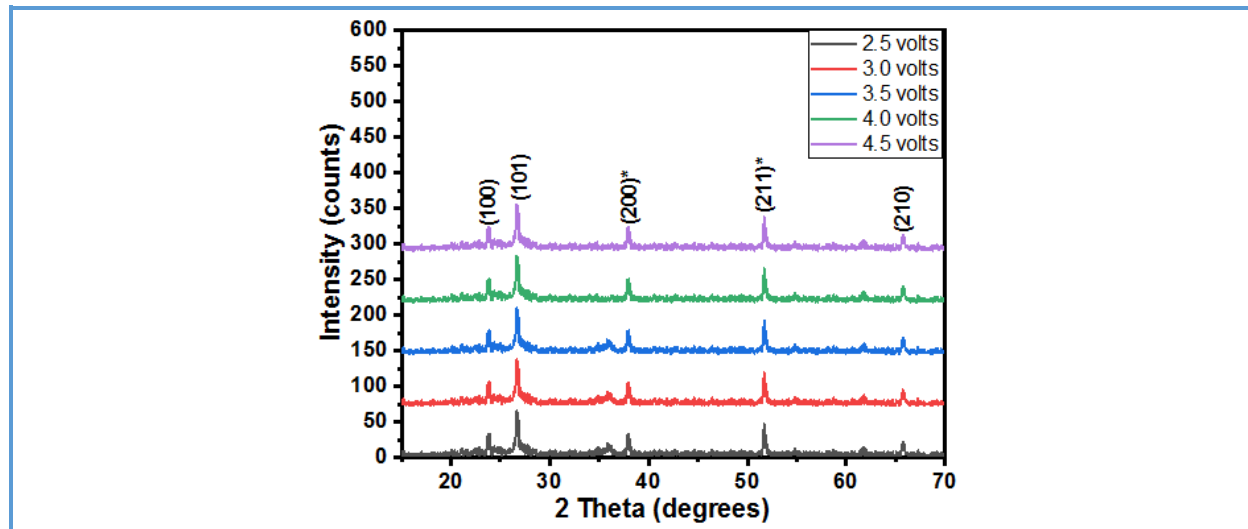
### KEYWORDS

Sb:ZnTe thin film  
Optoelectronic materials  
Electrodeposition  
Semiconductor alloys  
Energy band engineering

### ABSTRACT

Thin films of antimony-doped zinc telluride (Sb:ZnTe) were produced using an electrodeposition method. The examination included both the structural and optical characteristics, as well as the size of the crystallites. X-ray diffraction (XRD) analysis revealed Sb:ZnTe on Fluorine doped Tin Oxide (FTO) substrates had a hexagonal structure. The crystallite sizes in these thin films vary between 23.88 nm and 33.00 nm with dislocation density within the range of  $2.32$  to  $1.02 \times 10^{15}$  lines/m<sup>2</sup> and the microstrain between 5.59 and 3.99. UV-Vis spectroscopy revealed the absorbance values of the film decreased, with a range of 33% to 54% as the wavelength increased from 400 nm to 1100 nm. The transmittance and reflectance values of the film varied between 28.50% and 48.0% and less than 20.5%, respectively, suggesting that the deposited thin films are appropriate for use as antireflective coatings in smart window technology. The refractive indices of the films varied between 2.40 and 2.63. The extinction coefficient was found to increase with wavelength across the studied spectrum (400 nm to 1100 nm) and decrease with higher deposition potential. These extinction coefficient values suggest that the films are appropriate for use as absorber layers in thin-film solar cells. A band gap of 2.00 eV was determined at 2.5 volts and as the deposition potential increased, the films showed a decrease in the energy band gap. Gravimetric method analysis revealed that the thickness of antimony doped zinc telluride films increased from 126.18 nm to 378 nm as the deposition potentials increased from 2.5 volts to 4.5 volts. It is critical to control the electrodeposition potential to achieve the desired film thickness and properties.

## Graphical Abstract



## Introduction

As scientific inquiry progressed, thin films have emerged as materials with distinctive properties which significantly differ from their bulk counterparts. Over the past few years, the thorough understanding and modification of thin film properties has had a significant impact on their use in various electronic applications. Scientists have invested substantial resources in the synthesis of semiconducting thin films. The combination of elements from Group II (metals) and Group VI (chalcogens) on the periodic table [1] produces compounds that exhibit semiconductor properties. These semiconducting materials have generated a great deal of interest in both fundamental research and practical technological applications [2]. Among these compounds, those derived from Group IIB and Group VI elements, such as zinc based chalcogenides (ZnO, ZnS, ZnSe, and ZnTe) and cadmium based chalcogenides (CdO, CdS, CdSe, and CdTe), have been widely used in an array of optoelectronic devices such as radiation detectors, solar cells, magneto-optical devices, visible light photodetectors, LEDs, magneto-

optical devices, nonlinear optical materials, and others [3-14].

Zinc telluride (ZnTe) stands out as a leading material in this category of semiconductor compounds. The transparency of this p-type binary compound semiconductor to photons with energy levels below 2.26eV makes it an attractive choice for back contact with thin film solar cells [15-16]. ZnTe as a back contact in thin solar cells is aimed to enhance the overall performance of the solar cell by facilitating better light absorption and electron-hole pair generation within the thin film based solar cell configuration [17]. ZnTe is favoured for application in light-emitting diodes (LEDs) due to its advantageous direct band gap energy [18-20].

Furthermore, the band gap of ZnTe had been tuned by metal and non-metal ion doping such as Al [20-21], Sn [18,22-23], Cu [24-26], Sb [18,22,27-28], Bi [29], As [30], Cd [31-32], N [33], and P [34-35]. This possibility of tuning by dopants positioned ZnTe as potential candidate for various industrial applications. ZnTe thin films have been deposited using various techniques such as thermal evaporation [23,29,36-37], close space

sublimation (CSS) [38-39], glancing angle technique [40], chemical bath [19, 41-42], electrodeposition [43-47], pulsed laser deposition [48-49], reactive radiofrequency [33], metalorganic chemical vapor deposition (MOCVD) [30], and radio-frequency magnetron sputtering [50-51].

Electrochemical deposition, also known as electrodeposition or electroplating, is a versatile and widely used technique for depositing thin films and coatings onto conductive substrates. It involves the reduction of metal ions from a solution onto a conductive surface under the influence of an electric field [52]. This deposition technique presents several benefits, such as precise management of film characteristics, the ability to coat conformally, fast deposition rates, cost-effective, suitability for multicomponent setups, eco-friendliness and flexibility [53-54]. These factors make it a preferred choice for thin film fabrication in various fields, ranging from microelectronics and optoelectronics to corrosion protection and decorative coatings. Many researchers such as [55-62] have reported the use of electrodeposition in the synthesis of binary, ternary, and quaternary thin films.

The motivation for the work arose from the fact that there is no literature available on the impact of deposition potential on the structural and optical properties of electrodeposited antimony doped zinc telluride (Sb:ZnTe) thin films. Reports from literatures on antimony doped zinc telluride thin films as presented by [18,22,27-28] showed no information on the effect of deposition potential on the optical and structural properties of Sb:ZnTe thin films. The purpose of this research is to address this literature gap by investigating the effect of deposition potential on the structural and optical properties of Sb:ZnTe thin films synthesized via electrodeposition. Specifically,

we aim to elucidate how different deposition potentials influence the structural and optical properties of electrodeposited Sb:ZnTe thin films.

## Experimental

### *Reagents*

The electrodeposition of antimony-doped zinc telluride (Sb:ZnTe) involved the use of antimony trichloride ( $\text{SbCl}_3$ ) and zinc (II) acetate dihydrate ( $\text{Zn}(\text{CH}_3\text{CO}_2)_2 \cdot 2\text{H}_2\text{O}$ ) as precursors for antimony and zinc, respectively. Tellurium dioxide ( $\text{TeO}_2$ ) served as the precursor for telluride ions, sodium sulfate acted as the supporting electrolyte,  $\text{H}_2\text{SO}_4$  was used as pH adjuster and distilled water was utilized as the solvent medium.

### *Apparatus*

The experimental setup utilized various apparatus, including 100 mL beakers for solution mixing, fluorine-doped tin oxide (FTO) glass substrates as working electrodes, an electronic compact scale for precise reagent measurements, and a magnetic stirrer hotplate for solution agitation. The electric energy was delivered by a DC power supply while the potential and current of the deposition were measured using digital multimeters. The reference electrode was an Ag/AgCl electrode, while the counter electrode was a platinum rod. Substrate degreasing was accomplished using an ultrasonic bath, and drying during the post-deposition heat treatment was made easier by an electrical oven.

### *Material preparation*

Molar solutions of the reagents prepared for the deposition include:

(1) Zinc (II) acetate dihydrate solution (0.20 M): Dissolve 4.39 grams of zinc (II) acetate dihydrate in 100 milliliters of distilled water.

(2) Antimony trichloride solution (0.05 M): Dissolve 1.14 grams of antimony trichloride in 100 milliliters of distilled water.

(3) Tellurium (IV) oxide solution (0.10 M): Dissolve 1.60 grams of  $\text{TeO}_2$  in 100 milliliters of distilled water.

(4) Sodium sulphate ( $\text{Na}_2\text{SO}_4$ ) solution (0.05 M): Dissolve 8.06 grams of sodium sulphate in 500 milliliters of double-distilled water.

(5) Zinc (II) acetate dihydrate, antimony trichloride, tellurium dioxide aqueous solutions were used as precursors for Zn, Sb, and Te ions while sodium sulphate was employed as a supporting electrolyte. In addition, the pH of the electrolytic bath was adjusted using 1.0 M  $\text{H}_2\text{SO}_4$ .

#### Substrate pre-treatment

Four distinct processes were employed for the cleaning of fluorine-doped tin oxide (FTO) glass substrates before used in

electrodeposition of films. These four processes are depicted in [Figure 1](#).

#### Electrosynthesis of antimony doped zinc tellurium thin films

[Figure 2](#) illustrates the electrodeposition setup, which is made-up of the electrolyte, electrodes, and power supply unit. The electrodeposition setup of [63] was employed in this research work. As shown in [Figure 2](#), the configuration involved a three-electrode electrodeposition setup which are working, reference and counter electrodes.

The working electrode, serving as the cathode, was the conducting substrate (FTO). A platinum electrode was used as the anode (counter electrode). A reference electrode of Ag/AgCl was utilized in the deposition of the thin film. The electrodeposition setup was powered by the Dazheng digital DC-power supply unit (PS-1502A) model. Two digital multimeters (DT9201A CE and Mastech MY60) were employed to measure deposition potential and current, respectively.

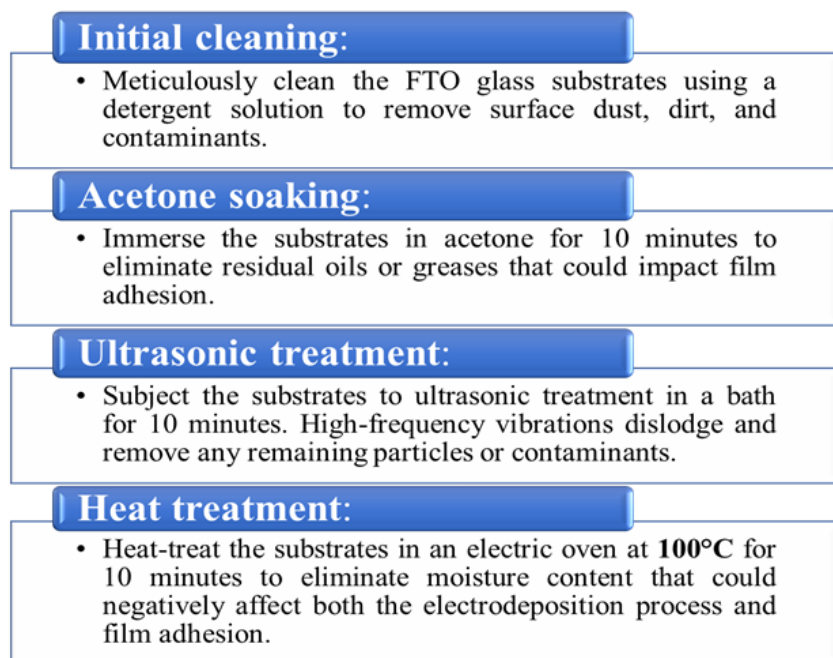


**Figure 1.** Pre-treatment steps for cleaning of FTO achieving optimal film quality.

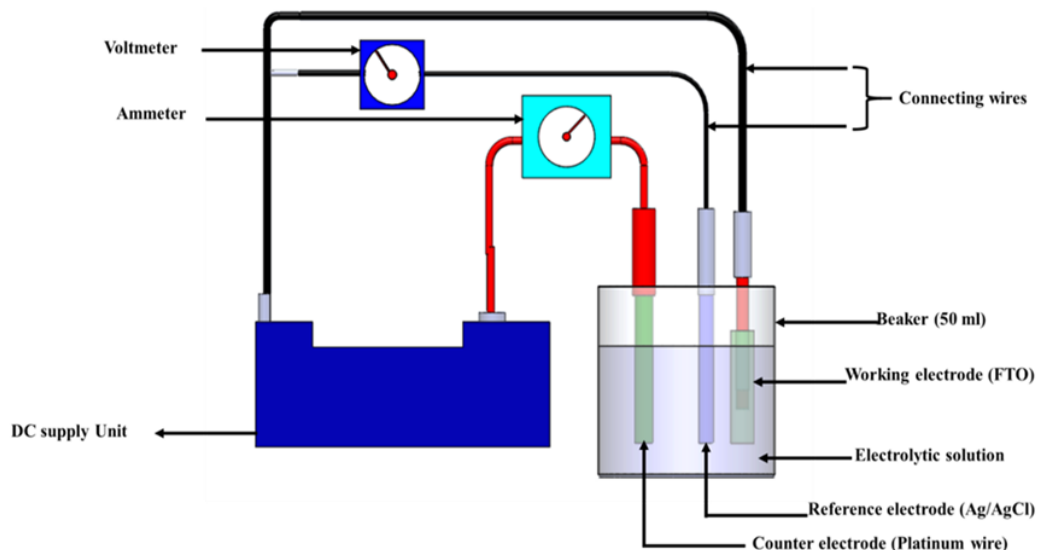
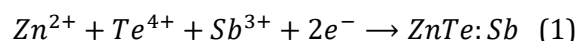


**Figure 2.** Schematic diagram of the electrodeposition experimental set up [63].

To deposit antimony doped zinc telluride thin films onto a FTO substrate using electrodeposition, a homogeneous aqueous electrolytic bath was formed by mixing 15 mL of 0.20 M zinc (II) acetate dihydrate, 10 mL of 0.05 M of antimony trichloride and 5 mL of concentrated 1 M of  $H_2SO_4$ . The mixture was properly mixed using a magnetic stirrer for a duration of 5 minutes. This follows with the addition of 15 mL of 0.10 M tellurium dioxide and 5 mL of 0.05 M  $Na_2SO_4$ . The resultant solution was employed after five more minutes of magnetic stirring. After that, the three electrodes were submerged in the electrolytic bath and kept at a steady 2.5-volt potential for precisely sixty seconds. To improve the characteristics of the deposited Sb:ZnTe thin film, the deposited layer was then thermally treated for 20 minutes at 100 °C. At various deposition potentials of 3.0, 3.5, 4.0, and 4.5 volts, four additional antimony-doped zinc telluride thin films were deposited. The mechanism of the formation of antimony doped zinc telluride is shown in Equation (1).



At the cathode (working electrode), Zinc ions ( $Zn^{2+}$ ), antimony ions ( $Sb^{3+}$ ), and tellurium ions ( $Te^{4+}$ ) were reduced through electron transfer which lead to the deposition of the Zn, Sb, and Te metals. The simultaneous reduction of zinc, tellurium, and antimony ions results in the formation of the compound Sb:ZnTe on the electrode surface.

#### *Characterization of deposited superlattice*

The deposited antimony doped zinc telluride thin films were subjected to film thickness measurement using gravimetric method. Optical, electrical, and structural properties were also studied. Optical properties were carried out using 756S UV-Vis spectrophotometer. Structural analysis of the films was obtained using Drawell x-ray diffractometer.

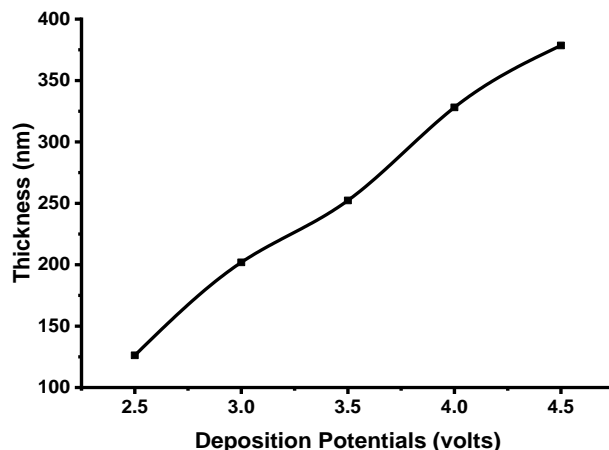


Figure 3. Graph of thickness against deposition potential.

## Results and Discussions

### Film thickness measurement

The thickness of the film was determined using the mass difference method, as described in Equation (2) in references [65-66].

$$t = \frac{\Delta m}{\rho A}, \quad (2)$$

Where, A is the area of the substrate covered by the deposited thin films,  $\rho$  is the bulk density of ZnTe (assumed to be  $6.34 \text{ g/cm}^3$ ), and  $\Delta m$  is the mass difference found by measuring the substrate mass before and after the deposition.

A graph of the thickness of Sb-doped ZnTe film plotted against the deposition potential is presented in Figure 3. As the deposition potentials rose from 2.5 volts to 4.5 volts, the film thickness went up from 126.18 nm to 378 nm. Controlling the electrodeposition potential is crucial for achieving the desired film thickness and properties. As the deposition potentials increases, faster reduction rates are experienced by the ions resulting in thicker films because more metal ions are being reduced and deposited. This result is similar to the increase in thickness as deposition potential increases as obtained by [67-68].

### Structural analysis

In Figure 4, the x-ray diffraction spectra of the thin films composed of Sb-doped ZnTe deposited on electrodes are presented. The diffractograms illustrate an x-ray pattern consistent with the hexagonal phase of ZnTe, as indicated by the JCPDS file number (00-019-1482). Structural phase of ZnTe obtained in this work is similar to those obtained by [69-70]. Equation (4) demonstrates how the Debye-Scherrer formula was used to calculate the crystallite sizes of the thin films that were deposited [71-72].

$$D = \frac{0.9 \lambda}{\beta \cos \theta} \quad (3)$$

Dislocation densities of the deposited Sb doped ZnTe were calculated using Equation (4) as given by [73-74].

$$\delta = \frac{1}{D^2} \quad (4)$$

Microstrains of the deposited Sb doped ZnTe were calculated using Equation (5), respectively, as given by [75-76].

$$\varepsilon = \frac{\beta}{4 \tan \theta} \quad (5)$$

Table 1 indicates the structural parameters of the Sb-doped ZnTe thin films that were deposited. In addition, Figures 5(a-c) illustrates the relationship between deposition



potential and key structural characteristics, namely crystallite size ( $d$ ), dislocation density ( $\delta$ ), and microstrain ( $\epsilon$ ). The crystallite size of the films ranges from 23.88 nm to 33.00 nm. The increase in crystallite size, as shown in Figure 5(a) often indicates improved structural phase. Larger crystallites generally have fewer grain boundaries. The increased crystalline structure of the films as a result of the higher deposition potential is responsible for the

observed heightened intensity. Figures 5 (b and c) demonstrate that when deposition potential increases, dislocation density, and microstrain trend downward. A decrease in microstrain and dislocation density points to a reduced density of crystal defects. A more well-organized and flawless crystal lattice is facilitated by fewer dislocations and reduced microstrain.

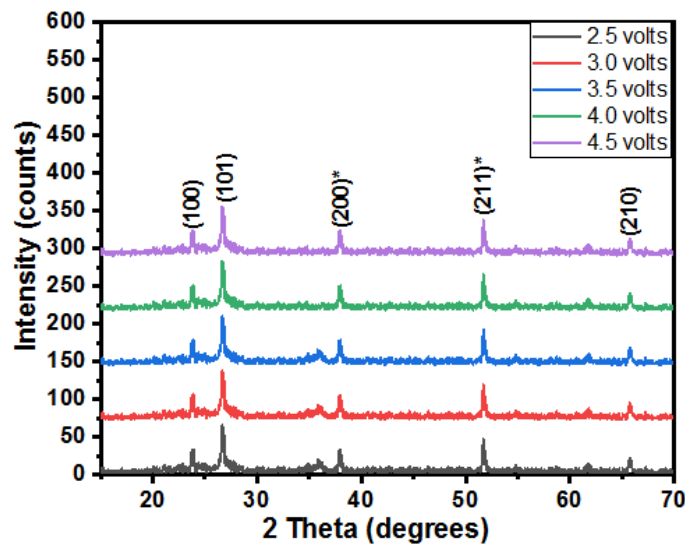


Figure 4. Diffractograms of antimony doped zinc telluride thin films deposited at varying potentials.

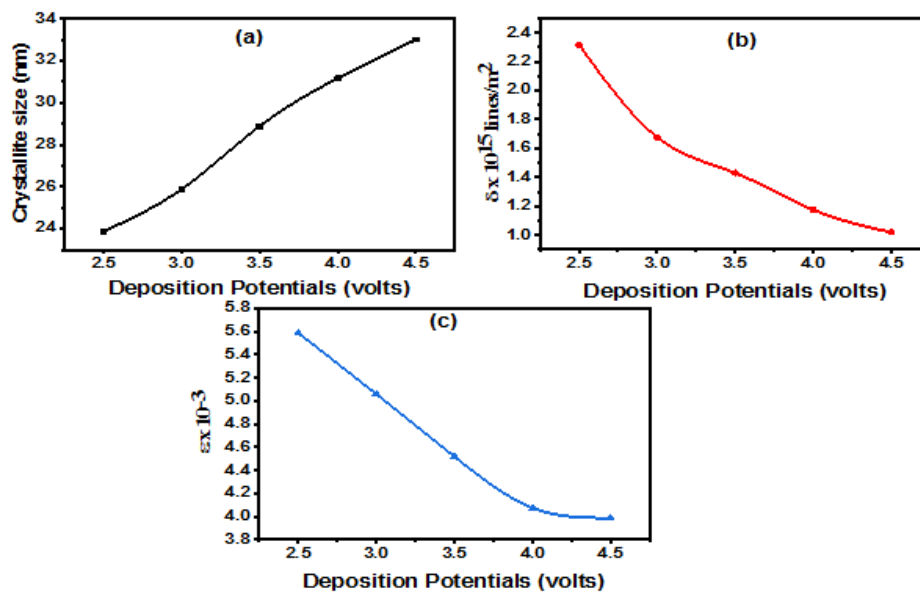


Figure 5. Variation of structural parameters (a) crystallite size ( $D$ ), (b) dislocation density ( $\delta$ ) and microstrain ( $\epsilon$ ) with deposition potentials.

**Table 1.** Structural parameters of electrodeposited antimony doped zinc telluride thin film

<b>2 <math>\theta</math> (<math>^{\circ}</math>)</b>	<b>d - spacing (nm)</b>	<b>FWHM (<math>^{\circ}</math>)</b>	<b>D (nm)</b>	<b><math>\delta \times 10^{15}</math> Lines/m<sup>2</sup></b>	<b><math>\epsilon \times 10^{-3}</math></b>
23.255	3.822	0.543	15.595	4.112	11.518
26.715	3.334	0.315	27.046	1.367	5.794
37.943	2.369	0.302	29.071	1.183	3.831
51.732	1.766	0.291	31.728	0.993	2.616
65.831	1.418	0.620	15.939	3.936	4.180
			<b>23.876</b>	<b>2.318</b>	<b>5.588</b>
23.823	3.732	0.391	21.46	2.172	8.175
26.715	3.334	0.408	20.91	2.287	7.495
37.943	2.369	0.395	22.22	2.026	5.013
51.732	1.766	0.285	32.39	0.953	2.562
65.775	1.419	0.305	32.43	0.951	2.056
			<b>25.92</b>	<b>1.678</b>	<b>5.060</b>
23.873	3.724	0.265	31.98	0.978	5.474
26.765	3.328	0.478	17.85	3.139	8.764
37.993	2.366	0.293	29.75	1.13	3.738
51.782	1.764	0.285	32.39	0.953	2.560
65.825	1.418	0.305	32.44	0.95	2.054
			<b>28.95</b>	<b>1.43</b>	<b>4.518</b>
23.847	3.728	0.248	34.16	0.857	5.129
26.739	3.331	0.412	20.70	2.334	7.564
37.967	2.368	0.238	36.88	0.735	3.018
51.756	1.765	0.287	32.10	0.97	2.584
65.799	1.418	0.309	31.98	0.978	2.084
			<b>31.17</b>	<b>1.175</b>	<b>4.076</b>
23.263	3.821	0.325	26.09	1.469	6.883
26.715	3.334	0.305	27.97	1.278	5.603
37.944	2.369	0.287	30.52	1.073	3.648
51.733	1.766	0.255	36.1	0.767	2.299
65.775	1.419	0.223	44.32	0.509	1.504
			<b>33.00</b>	<b>1.019</b>	<b>3.987</b>

### Optical analysis

UV-Vis spectroscopy was employed to analyse the optical properties of electrodeposited thin films of antimony-doped zinc telluride (ZnTe) across a wavelength range of 400 nm to 1100 nm. The choice of the wavelength is because this range corresponds to the visible and near-infrared (NIR) regions of the electromagnetic

spectrum. As depicted in [Figure 6](#), the absorbance of the antimony-doped ZnTe thin films exhibits a decline as the wavelength increases from 400 nm to 1100 nm. Moreover, a rise in absorbance is observed with an increase in the deposition potential from 2.5 volts to 4.5 volts. The absorbance values were observed to vary between 33% and 54%.



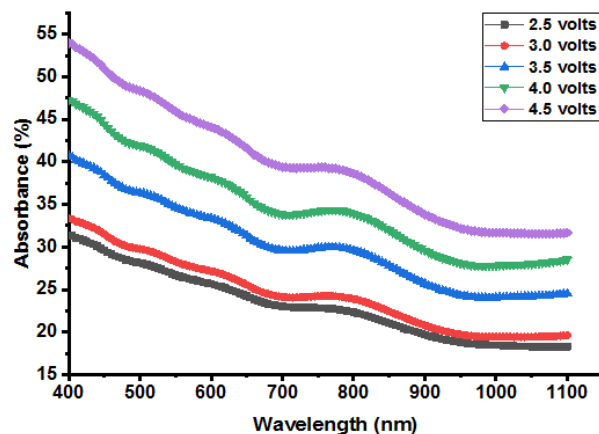


**Figure 6.** Absorbance spectra as a function of wavelength for antimony-doped zinc telluride (Sb:ZnTe) thin films at varied deposition potentials.

The graph in [Figure 7](#) depicts transmittance spectra plotted against wavelength. As the wavelength increases from 400 nm to 1100 nm, the transmittance values of the films also increase. However, when the deposition potential increases, the transmittance decreases. These films exhibit moderate transmittance within the visible (VIS) region and high transmittance within the near-infrared (NIR) region, with transmittance values ranging from 28.50% to 48.0%.

[Figure 8](#) depicts the reflectance spectra of the films plotted against wavelength from 400 nm to 1100 nm. The reflectance values of the deposited thin films were consistently lower than 20.5%. The spectra illustrate a continuous decrease in reflectance as the wavelength increases for deposition potentials of 2.5 volts

and 3.0 volts. With increasing deposition potential, reflectance is observed to rise within the VIS region and decline within the NIR region. Minimal reflectance values were observed within the NIR regions, indicating suitability for antireflective coating in smart window applications [65].

[Figure 9](#) presents a graph of refractive index plotted against wavelength at different deposition potentials. The refractive indices of the films fall within the range of 2.40 to 2.63. Interestingly, the refractive index values decrease as the wavelength increases. However, when the deposition potential varies from 2.5 to 3.0 volts, the refractive index increases, and then it decreases again from 3.5 volts to 4.5 volts.

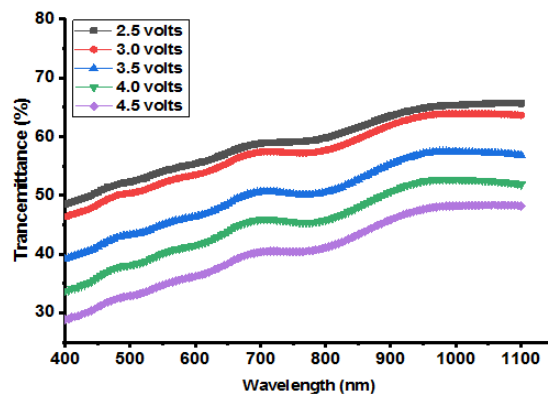


**Figure 7.** Transmittance spectra as a function of wavelength for antimony-doped zinc telluride (Sb:ZnTe) thin films at varied deposition potentials.

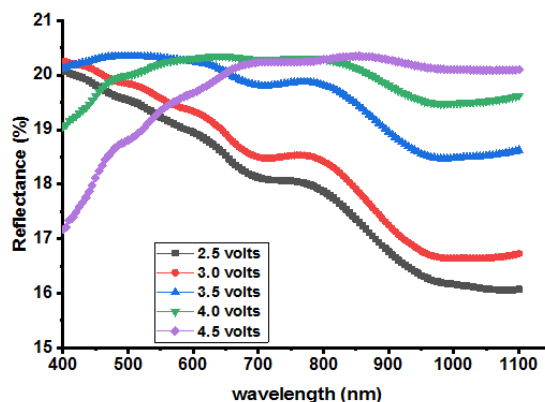


**Figure 8.** Reflectance spectra as a function of wavelength for antimony-doped zinc telluride (Sb:ZnTe) thin films at varied deposition potentials.

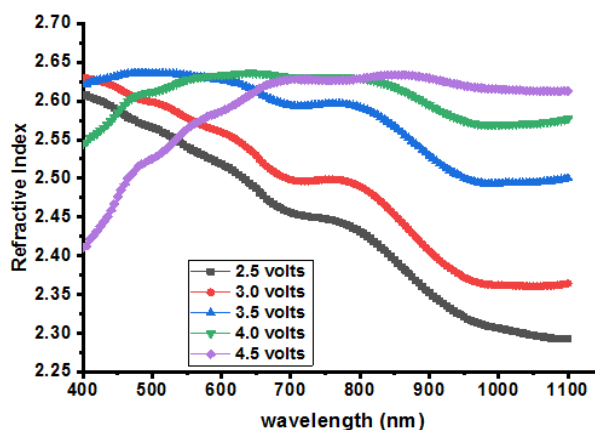


**Figure 9.** Refractive index as a function of wavelength for antimony-doped zinc telluride (Sb:ZnTe) thin films at varied deposition potentials.

Figure 10 displays the graph depicting the extinction coefficient ( $k$ ) of antimony-doped zinc telluride thin films. The values were observed to rise with increasing wavelength across the studied spectrum (400 nm to 1100 nm) and decrease with higher deposition potential. Within the visible (VIS) region (400 nm to 700 nm),  $k$  values of the thin films ranged from 1.85 to 1.03, indicating effective photon energy absorption. Specifically, at deposition potentials of 2.5 volts, 3.0 volts, 3.5 volts, 4 volts, and 4.5 volts,  $k$  values ranged from 1.85 to 2.93, 1.24 to 1.97, 1.21 to 1.96, 1.04 to 1.75, and 1.03 to 1.68, respectively. The  $k$  measures the light absorption strength at a given wavelength. The spectrum of extinction

coefficient values verifies the suitability of these films for application as absorber layers in thin-film solar cells.

In Figure 11, the relationship between  $(\alpha h\nu)^2$  and photon energy is demonstrated for antimony-doped zinc telluride (Sb:ZnTe) thin films deposited at different deposition potentials. By extrapolating the linear part of the graph along the photon energy axis, the energy band gaps of these films were estimated. Specifically, a band gap of 2.00 eV was obtained for antimony-doped zinc telluride thin film deposited at 2.5 volts. For films deposited at 3.0 volts, 3.5 volts, 4.0 volts and 4.5 volts, the band gaps were found to be 1.95 eV, 1.90 eV, 1.90 eV, and 1.85 eV,

respectively. These results indicate a decrease in the energy band gap of the films as the deposition potential increases, suggesting the possible adjustment of energy band gap of antimony-doped zinc telluride by varying the deposition potential. These findings suggest

that as the deposition potential increases, there is a decrease in the energy band gap of the films, implying the possibility of adjusting the energy band gap of antimony-doped zinc telluride by varying the deposition potential.

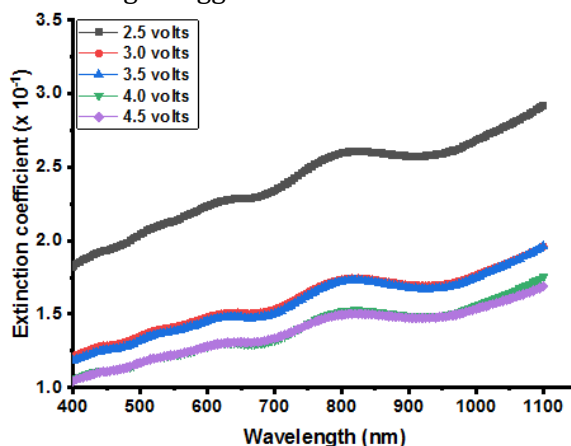


**Figure 10.** Extinction coefficient as a function of wavelength for antimony-doped zinc telluride (Sb:ZnTe) thin films at varied deposition potentials

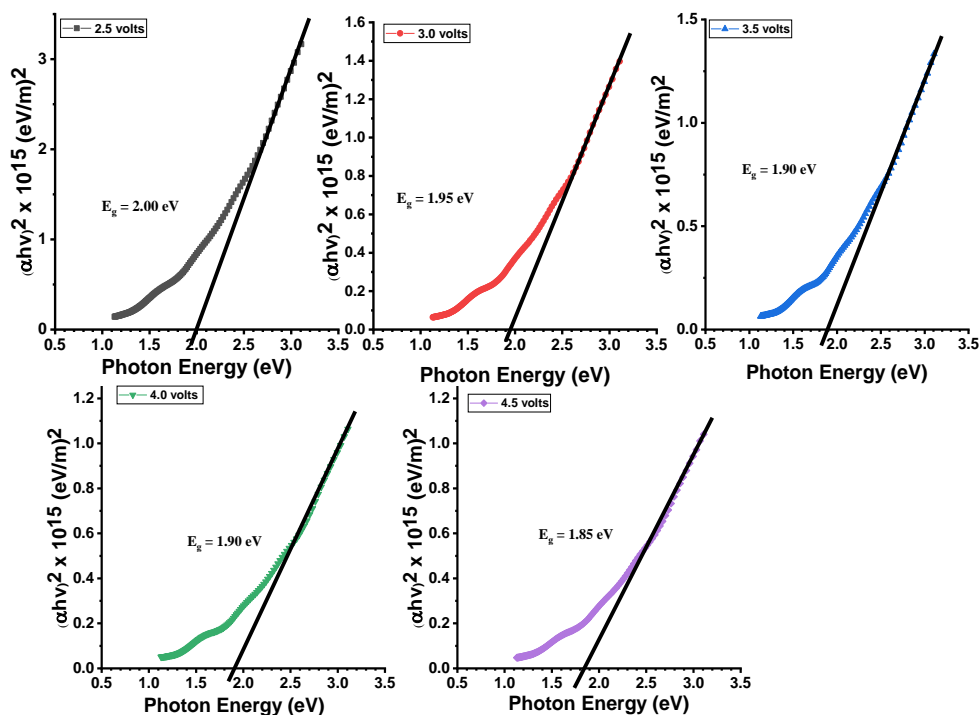


**Figure 11.**  $(\alpha h\nu)^2$  as a function of wavelength for antimony-doped zinc telluride (Sb:ZnTe) thin films at varied deposition potentials

These range of energy bandgap values positioned Sb:ZnTe thin films as potential materials for top junction (absorber layer) of a multijunction solar cells. The decrease in band gap of the Sb:ZnTe thin films as deposition potential increased from 2.5 volts to 4.5 volts could be attributed to improvement in the crystallinity and structural defects in the deposited films. These changes in grain size and crystallinity can impact the electronic band structure thereby modifying the band gap of the films. [75,77-79] have reported similar decrease in energy band gap of thin films as deposition potentials increases.


## Conclusion

To sum up, the investigation into the electrodeposited antimony-doped zinc telluride (Sb:ZnTe) thin films has provided valuable insights into the influence of deposition potential on their structural and optical properties. The observed increase in film thickness, ranging from 126.18 nm to 378.55 nm, as the deposition potentials increased from 2.5 volts to 4.5 volts, underscores the critical role of control in achieving the desired film characteristics. Structural analysis done with X-ray diffraction, not only confirmed the hexagonal phase of ZnTe, but also revealed a substantial enhancement in crystallite size, ranging from 23.88 nm to 33.00 nm, and a simultaneous decrease in dislocation density and microstrain with higher deposition potential. The optical properties exhibited distinctive trends, with absorbance values ranging from 33% to 54%, transmittance from 28.50% to 48.0%. The energy band gap demonstrated tunability, decreasing from 2.00 eV at 2.5 volts to 1.85 eV at 4.5 volts.

The optical properties, characterized by tunable energy band gaps, absorbance values,

and high transmittance in the near-infrared region, indicate the potential suitability of these films for applications in solar energy harvesting, antireflective coatings, and transparent conductive coatings. The refractive indices spanning 2.40 to 2.63 further hint at their use in optical devices requiring controlled refractive properties. These distinction findings underscore the pivotal role of deposition potential in tailoring Sb:ZnTe thin films for specific applications, providing quantifiable insights into their optimization for thin-film solar cells, antireflective coatings, and the other optoelectronic devices.

## Orcid

Victor Chukwuagozie Onuabuchi : 0000-0002-8373-5859

## References

- [1]. Nande, A., Kalyani, N. T., Tiwari, A., Dhoble, S. J. Exploring the world of functional materials. In *Functional Materials from Carbon, Inorganic, and Organic Sources* Woodhead Publishing Series in Electronic and Optical Materials, Woodhead Publishing, 2023, pp 1-19 [[Crossref](#)]
- [2]. Hossain N., Mobarak M.H., Mimona M.A., Islam M.A., Hossain A., Zohur F.T., Chowdhury M.A. Advances and significances of nanoparticles in semiconductor applications–A review, *Results in Engineering*, 2023, 101347 [[Crossref](#)], [[Google Scholar](#)], [[Publisher](#)]
- [3]. Shen Y., Zhang Y., Huo J., Li X., Yan Z., Pan Y., Sun W., Deng N., Kang W., Two-dimensional SnSe material for solar cells and rechargeable batteries, *Journal of Energy Storage*, 2023, 69:107958 [[Crossref](#)], [[Google Scholar](#)], [[Publisher](#)]
- [4]. Lal N., Chawla K., Sharma S., Chouhan R.L., Lal C. Study of electrodeposited zinc selenide (ZnSe) nanostructure thin films for solar cell

- applications, *Journal of the Indian Chemical Society*, 2023, **100**:101006 [[Crossref](#)], [[Google Scholar](#)], [[Publisher](#)]
- [5]. Campbell S., Phillips L.J., Major J.D., Hutter O.S., Voyce R., Qu Y., Beattie N.S., Zoppi G., Barrioz V. Routes to increase performance for antimony selenide solar cells using inorganic hole transport layers, *Frontiers in Chemistry*, 2022, **10**:954588 [[Crossref](#)], [[Google Scholar](#)], [[Publisher](#)]
- [6]. Chen X., Li J., Zhong Y., Li X., Pan M., Qi H., Dong H., Zhang L. Highly efficient and stable CdZnSeS/ZnSeS quantum dots for application in white light-emitting diode, *Frontiers in Chemistry*, 2022, **10**:845206 [[Crossref](#)], [[Google Scholar](#)], [[Publisher](#)]
- [7]. Zargar R.A. Fabrication and improved response of ZnO-CdO composite films under different laser irradiation dose, *Scientific Reports*, 2022, **12**:10096 [[Crossref](#)], [[Google Scholar](#)], [[Publisher](#)]
- [8]. Gozeh B.A., Karabulut A., Yildiz A., Dere A., Arif B., Yakuphanoglu F. SILAR controlled CdS nanoparticles sensitized CdO diode based photodetectors, *Silicon*, 2020, **12**:1673 [[Crossref](#)], [[Google Scholar](#)], [[Publisher](#)]
- [9]. Bairy R., Somayaji A., Marakala N., Devadiga U., Rajesh M., Wal J.C. Role of Cobalt Doping on the Physical Properties of CdO Nanocrystalline Thin Films for Optoelectronic Applications, *Advances in Materials Science and Engineering*, 2022, **2022**: [[Crossref](#)], [[Google Scholar](#)], [[Publisher](#)]
- [10]. Patra P., Kumar R., Kumar C., Mahato P.K. Ni-incorporated cadmium sulphide quantum dots for solar cell: an evolution to microstructural and linear-nonlinear optical properties, *Journal of Crystal Growth*, 2022, **583**:126542 [[Crossref](#)], [[Google Scholar](#)], [[Publisher](#)]
- [11]. Rashid M.H., Koel A., Rang T., Nasir N., Sabir N., Ameen F., Rasheed A. Optical dynamics of copper-doped cadmium sulfide (CdS) and zinc sulfide (ZnS) quantum-dots core/shell nanocrystals, *Nanomaterials*, 2022, **12**:2277 [[Crossref](#)], [[Google Scholar](#)], [[Publisher](#)]
- [12]. Feng H., Song J., Song B., Lin Q., Shen H., Li L.S., Wang H., Du Z. Highly efficient near-infrared light-emitting diodes based on chloride treated CdTe/CdSe type-II quantum dots, *Frontiers in Chemistry*, 2020, **8**:266 [[Crossref](#)], [[Google Scholar](#)], [[Publisher](#)]
- [13]. Grover R., Srivastava R., Saxena K. Luminescence studies in cadmium telluride nanocrystals grown on glass substrates, *RSC Advances*, 2022, **12**:26596 [[Crossref](#)], [[Google Scholar](#)], [[Publisher](#)]
- [14]. Elmourabit F., Dlimi S., Ouissaaden F.I., Khoukh A., Amiri L., Nkhaili L., Limouny L., Narjis A. Structural and optical properties of smooth radio frequency sputtered XTe (X= Cd, Zn) thin films, *Physica B: Condensed Matter*, 2023, **666**:415058 [[Crossref](#)], [[Google Scholar](#)], [[Publisher](#)]
- [15]. Isik M., Gullu H., Parlak M., Gasanly N. Synthesis and temperature-tuned band gap characteristics of magnetron sputtered ZnTe thin films, *Physica B: Condensed Matter*, 2020, **582**:411968 [[Crossref](#)], [[Google Scholar](#)], [[Publisher](#)]
- [16]. Mahmood A., Rashid R., Aziz U., Shah A., Ali Z., Raza Q., Ashraf T. Structural and optical properties of Zn<sub>1-x</sub>Ni<sub>x</sub>Te thin films prepared by electron beam evaporation technique, *Progress in Natural Science: Materials International*, 2015, **25**:22 [[Crossref](#)], [[Google Scholar](#)], [[Publisher](#)]
- [17]. Suthar D., Chuhadiya S., Sharma R., Dhaka M. An overview on the role of ZnTe as an efficient interface in CdTe thin film solar cells: a review, *Materials Advances*, 2022, **3**:8081 [[Crossref](#)], [[Google Scholar](#)], [[Publisher](#)]
- [18]. Pandey N., Kumar B., Dwivedi D. Synthesis and characterization of pure and Sb/Sn doped ZnTe for solar cell application, *Materials*

- Research Express*, 2019, **6**:096425 [[Crossref](#)], [[Google Scholar](#)], [[Publisher](#)]
- [19]. Younus I.A., Ezzat A.M., Uonis M.M. Preparation of ZnTe thin films using chemical bath deposition technique, *Nanocomposites*, 2020, **6**:165 [[Crossref](#)], [[Google Scholar](#)], [[Publisher](#)]
- [20]. Maki S.A., Hassun H.K. Effect of Aluminum on Characterization of ZnTe/n-Si Heterojunction Photodetector, *Journal of Physics: Conference Series*, (IOP Publishing), **2018**, *1003*, 012085. [[Crossref](#)], [[Google Scholar](#)], [[Publisher](#)]
- [21]. Jang Y.J., Lee C., Moon Y.H., Choe S. Solar-Driven Syngas Production Using Al-Doped ZnTe Nanorod Photocathodes, *Materials*, 2022, **15**:3102 [[Crossref](#)], [[Google Scholar](#)], [[Publisher](#)]
- [22]. Chamola P., Mittal P. Impact of ZnTe, SbZnTe and SnZnTe absorber materials for multi-layered solar cell: parametric extraction and layer wise internal analysis, *Optik*, 2020, **224**:165626 [[Crossref](#)], [[Google Scholar](#)], [[Publisher](#)]
- [23]. Pandey N., Kumar B., Dwivedi D.K. Structural and optical properties investigation of Sn-doped ZnTe thin film, *Journal of Nano Trends - A Journal of Nano Technology & Its Applications*, 2019, **21**:13
- [24]. Lin X., Zhang Y., Zhu Z., Wu Q., Liu X. Radio frequency sputtered films of copper-doped zinc telluride, *Chemical Physics Letters*, 2021, **767**:138358 [[Crossref](#)], [[Google Scholar](#)], [[Publisher](#)]
- [25]. Ahmed M., Alshahrie A., Shaaban E.R. Resulting effect of the p-Type of ZnTe: Cu thin films of the intermediate layer in heterojunction solar cells: structural, optical, and electrical characteristics, *Materials*, 2023, **16**:3082 [[Crossref](#)], [[Google Scholar](#)], [[Publisher](#)]
- [26]. Kindvall A., Munshi A., Shimpi T., Danielson A., Sampath W.S. Copper-Doped Zinc Telluride Thin-Films as a Back Contact for Cadmium Telluride Photovoltaics. In *2018 IEEE 7th World Conference on Photovoltaic Energy Conversion (WCPEC) (A Joint Conference of 45th IEEE PVSC, 28th PVSEC & 34th EU PVSEC)*, 2018, 2994-2997. [[Crossref](#)], [[Google Scholar](#)], [[Publisher](#)]
- [27]. Barati A., Klein A., Jaegermann W. Deposition and characterization of highly p-type antimony doped ZnTe thin films, *Thin Solid Films*, 2009, **517**:2149 [[Crossref](#)], [[Google Scholar](#)], [[Publisher](#)]
- [28]. Mohanraj K., Thangarasu R., Mohanbabu B., Babu B. Preparation and characterization of nano sized pure ZnTe and antimony doped ZnTe nano thin films by spray pyrolysis technique, *Nanoscale Reports*, 2018, **1**:1 [[Crossref](#)], [[Google Scholar](#)]
- [29]. Das S., Priyadarshini P., Senapati S., Bisoyi S., Samal S., Naik R. Templet-free one-pot synthesis of Bi-doped ZnTe nanoflowers by cation exchange method for optoelectronic applications and antibacterial activity, *Journal of Alloys and Compounds*, 2023, **960**:170999 [[Crossref](#)], [[Google Scholar](#)], [[Publisher](#)]
- [30]. Oklobia O., Kartopu G., JC Irvine S. Properties of arsenic-doped ZnTe thin films as a back contact for CdTe solar cells, *Materials*, 2019, **12**:3706 [[Crossref](#)], [[Google Scholar](#)], [[Publisher](#)]
- [31]. Mahdy I.A., Mahmoud S.A., Mahdy M.A. Tuning structural, electrical, linear, and nonlinear optical properties of cadmium zinc telluride quantum dot thin films, *Journal of Materials Research*, 2023, **38**:391 [[Crossref](#)], [[Google Scholar](#)], [[Publisher](#)]
- [32]. Shah N.A., Mahmood W., Abbas M., Nazar N., Khosa A.H., Zeb A., Malik A. The synthesis of CdZnTe semiconductor thin films for tandem solar cells, *RSC Advances*, 2021, **11**:39940 [[Crossref](#)], [[Google Scholar](#)], [[Publisher](#)]
- [33]. Shimpi T.M., Drayton J., Swanson D.E., Sampath W.S. Properties of nitrogen-doped



- zinc telluride films for back contact to cadmium telluride photovoltaics, *Journal of Electronic Materials*, 2017, **46**:5112 [[Crossref](#)], [[Google Scholar](#)], [[Publisher](#)]
- [34]. Aqilia A., Abu-Omara T., Al-Reyahia A., Shaheena A., Al-Omaria S., Alhagisha I. Effect of phosphoric acid treatment on the physical properties of zinc telluride thin films, *Chalcogenide Letters*, 2023, **20**:113 [[Crossref](#)], [[Google Scholar](#)], [[Publisher](#)]
- [35]. Mustofa M., Mishima S., Saito K., Guo Q., Tanaka T. Growth of phosphorus-doped ZnTe thin films by molecular beam epitaxy using InP as the dopant source, *Japanese Journal of Applied Physics*, 2023, **62**:SK1031 [[Crossref](#)], [[Google Scholar](#)], [[Publisher](#)]
- [36]. Rehman K.M.U., Liu X., Riaz M., Yang Y., Feng S., Khan M.W., Ahmad A., Shezad M., Wazir Z., Ali Z. Fabrication and characterization of Zinc Telluride (ZnTe) thin films grown on glass substrates, *Physica B: Condensed Matter*, 2019, **560**:204 [[Crossref](#)], [[Google Scholar](#)], [[Publisher](#)]
- [37]. Athab R., Hussein B. Fabrication and investigation of zinc telluride thin films, *Chalcogenide Letters*, 2023, **20**:477 [[Crossref](#)], [[Google Scholar](#)]
- [38]. Lungu I., Ghimpu L., Untila D., Potlog T. Copper-related defects in ZnTe thin films grown by the close space sublimation method, *Moldavian Journal of the Physical Sciences*, 2022, **21**:34 [[Crossref](#)], [[Google Scholar](#)], [[Publisher](#)]
- [39]. Mahmood W., Awan S.U., Ud Din A., Ali J., Nasir M.F., Ali N., ul Haq A., Kamran M., Parveen B., Rafiq M., Pronounced impact of p-type carriers and reduction of bandgap in semiconducting ZnTe thin films by Cu doping for intermediate buffer layer in heterojunction solar cells, *Materials*, 2019, **12**:1359 [[Crossref](#)], [[Google Scholar](#)], [[Publisher](#)]
- [40]. Zarei R., Ehsani M., Dizaji H.R. An investigation on structural and optical properties of nanocolumnar ZnTe thin films grown by glancing angle technique, *Materials Research Express*, 2020, **7**:026419 [[Crossref](#)], [[Google Scholar](#)], [[Publisher](#)]
- [41]. Rathod K.C., Kamble P.D., Sanadi K.R., Kamble G.S., Guar M.L., Garadkar K.M. Photovoltaic application study of zinc telluride thin films grown by chemical bath deposition method, *Advances in Materials Physics and Chemistry*, 2021, **11**:131 [[Crossref](#)], [[Google Scholar](#)], [[Publisher](#)]
- [42]. Saeed N., Uonis M. Preparation of zinc telluride thin films using chemical bath deposition, *Chalcogenide Letters*, 2022, **19**:61 [[Crossref](#)], [[Google Scholar](#)]
- [43]. Seo J., Yoon S., Park K., Park J.J., Kim J., Yoo B. Role of Tellurium Ions for Electrochemically Synthesized Zinc Telluride 2D Structures on Nonconductive Substrate, *Advanced Materials Interfaces*, 2023, **10**:2202023 [[Crossref](#)], [[Google Scholar](#)], [[Publisher](#)]
- [44]. Luo M.s., Ma Z.w., Zhang Z.l., Wang Z.j., Jiang L.x., Jia M., Liu F.y. Preparation of semiconductor zinc telluride by photoelectrochemical deposition, *Journal of Central South University*, 2022, **29**:2899 [[Crossref](#)], [[Google Scholar](#)], [[Publisher](#)]
- [45]. Elsayed E., Shenouda A.Y. Studies on electrodeposition of zinc selenide and zinc telluride and their photoelectrochemical cell behavior, *Egyptian Journal of Chemistry*, 2022, **65**:623 [[Crossref](#)], [[Google Scholar](#)], [[Publisher](#)]
- [46]. Rajpal S., Kumar S. Annealing temperature dependent structural and optical properties of nanocrystalline ZnTe thin films developed by electrodeposition technique, *Solid State Sciences*, 2020, **108**:106424 [[Crossref](#)], [[Google Scholar](#)], [[Publisher](#)]
- [47]. Olusola O.I.O., Madugu M.L., Dharmadasa I.M., Growth of n-and p-type ZnTe semiconductors by intrinsic doping, *Materials*

- Research Innovations*, 2015, **19**:497 [[Crossref](#)], [[Google Scholar](#)], [[Publisher](#)]
- [48]. Faydh T.I., Salim K.D., Mahmood K.H. Structural and optical properties of manganese doped ZnTe: mn thin films prepared by pulsed laser method, *Journal of Pharmaceutical Negative Results*, 2022, 214 [[Crossref](#)], [[Google Scholar](#)], [[Publisher](#)]
- [49]. Ochoa-Estrella F., Vera-Marquina A., Mejia I., Leal-Cruz A., Pintor-Monroy M., Quevedo-López M. Structural, optical, and electrical properties of ZnTe: Cu thin films by PLD, *Journal of Materials Science: Materials in Electronics*, 2018, **29**:20623 [[Crossref](#)], [[Google Scholar](#)], [[Publisher](#)]
- [50]. Panaitescu A.M., Antohe I., Răduță A.M., Iftimie S., Antohe Ș., Mihăilescu C.N., Antohe V.A. Morphological, optical, and electrical properties of RF-sputtered zinc telluride thin films for electronic and optoelectronic applications, *AIP Advances*, 2022, **12**: 115013 [[Crossref](#)], [[Google Scholar](#)], [[Publisher](#)]
- [51]. Manica D., Antohe V.A., Moldovan A., Pascu R., Iftimie S., Ion L., Sucheș M.P., Antohe Ș. Thickness Effect on Some Physical Properties of RF Sputtered ZnTe Thin Films for Potential Photovoltaic Applications, *Nanomaterials*, 2021, **11**:2286 [[Crossref](#)], [[Google Scholar](#)], [[Publisher](#)]
- [52]. Costa J.G.d.R.d., Costa J.M., Almeida Neto A.F.d. Progress on electrodeposition of metals and alloys using ionic liquids as electrolytes, *Metals*, 2022, **12**:2095 [[Crossref](#)], [[Google Scholar](#)], [[Publisher](#)]
- [53]. Yu Y., Gong M., Dong C., Xu X. Thin-film deposition techniques in surface and interface engineering of solid-state lithium batteries, *Next Nanotechnology*, 2023, 100028 [[Crossref](#)], [[Google Scholar](#)], [[Publisher](#)]
- [54]. Ruiz-Gómez S., Fernández-González C., Perez L. Electrodeposition as a tool for nanostructuring magnetic materials, *Micromachines*, 2022, **13**:1223 [[Crossref](#)], [[Google Scholar](#)], [[Publisher](#)]
- [55]. Yimamu A., Afrassa M., Dejene B., Echendu O., Terblans J., Swart H., Motloug S. Electrodeposition of CdTe thin films using an acetate precursor for solar energy application: The effect of deposition voltage, *Materials Today Communications*, 2023, **35**:105673 [[Crossref](#)], [[Google Scholar](#)], [[Publisher](#)]
- [56]. Park J., Seo J., Lim J.H., Yoo B. Synthesis of copper telluride thin films by electrodeposition and their electrical and thermoelectric properties, *Frontiers in Chemistry*, 2022, **10**:799305 [[Crossref](#)], [[Google Scholar](#)], [[Publisher](#)]
- [57]. Sawant J., Bhujbal P., Choure N., Kale R., Pathan H. Copper indium disulfide thin films: electrochemical deposition and properties, *ES Materials & Manufacturing*, 2022, **17**:14 [[Crossref](#)], [[Google Scholar](#)]
- [58]. N'guessan A.I., Bouich A., Soro D., Soucase B.M. Growth of copper indium diselenide ternary thin films (CuInSe<sub>2</sub>) for solar cells: Optimization of electrodeposition potential and pH parameters, *Heliyon*, 2023, **9**: e19057 [[Crossref](#)], [[Google Scholar](#)], [[Publisher](#)]
- [59]. Mohapi T., Yimamu A., Tshabalala K., Motloug S. Effect of deposition voltage on the properties of electrodeposited CdZrS thin films for solar cell application, *Physica B: Condensed Matter*, 2023, **671**:415405 [[Crossref](#)], [[Google Scholar](#)], [[Publisher](#)]
- [60]. Tanwar A., Kaur R., Padmanathan N., Razeeb K.M. Electrodeposited CuSbTe thin films with enhanced thermoelectric performance, *Sustainable Energy & Fuels*, 2023, **7**:4160 [[Crossref](#)], [[Google Scholar](#)], [[Publisher](#)]
- [61]. Hwang S.K., Yoon J.H., Kim J.Y. Current Status and Future Prospects of Kesterite Cu<sub>2</sub>ZnSn (S, Se) <sub>4</sub> (CZTSSe) Thin Film Solar Cells Prepared via Electrochemical Deposition,

*ChemElectroChem*, 2024, e202300729 [Crossref], [Google Scholar], [Publisher]

[62]. Rodríguez-Rosales K., Marasamy L., Quiñones-Galván J., Santos-Cruz J., Mayén-Hernández S., Guillen-Cervantes A., Contreras-Puente G., de Moure-Flores F. One-step electrodeposition of CuAlGaSe<sub>2</sub> thin films using triethanolamine as a complexing agent, *Thin Solid Films*, 2020, **713**:138351 [Crossref], [Google Scholar], [Publisher]

[63]. Ezenwaka L., Okoli N., Okereke N., Ezenwa I., Nwori N., Properties of electrosynthesized cobalt doped zinc selenide thin films deposited at varying time, *Nanoarchitectonics*, 2022, 1 [Crossref], [Google Scholar], [Publisher]

[64]. Nwanya A.C., Obi D., Osuji R.U., Bucher R., Maaza M., Ezema F.I. Simple chemical route for nanorod-like cobalt oxide films for electrochemical energy storage applications, *Journal of Solid State Electrochemistry*, 2017, **21**:2567 [Crossref], [Google Scholar], [Publisher]

[65]. Nkamuo C., Okoli N., Nzekwe F., Egwunyenga N. Tuning the properties of manganese-doped zinc oxide nanostructured thin films deposited by SILAR approach, *Chemistry of Inorganic Materials*, 2024, **2**:100038 [Crossref], [Google Scholar], [Publisher]

[66]. Okoli N., Nkamuo C., Elekalachi C., Obimma I. Influence of Annealing Temperature on the Optical, Structural, Morphological and Compositional Properties of SILAR Deposited Copper Manganese Oxide Thin Films, *Journal of Nano and Materials Science Research*, 2022, **1**:68 [Google Scholar], [Publisher]

[67]. Wijanarka W.A., Toifur M. Effect of deposition voltage on layer thickness, microstructure, Cu/Ni sheet resistivity of deposition results by magnetic field electroplating assisted technique, *Indonesian*

*Review of Physics*, 2020, **3**:23 [Crossref], [Google Scholar], [Publisher]

[68]. Arulkumar E., Thanikaikarasan S., Tesfie N. Influence of deposition parameters for Cu<sub>2</sub>O and CuO thin films by electrodeposition technique: a short review, *Journal of Nanomaterials*, 2023, **2023** [Crossref], [Google Scholar], [Publisher]

[69]. Olusola O., Madugu M., Abdul-Manaf N., Dharmadasa I. Growth and characterisation of n-and p-type ZnTe thin films for applications in electronic devices, *Current Applied Physics*, 2016, **16**:120 [Crossref], [Google Scholar], [Publisher]

[70]. Olusola O.I.O., Madugu M.L., Dharmadasa I.M. Growth of n-and p-type ZnTe semiconductors by intrinsic doping, *Materials Research Innovations*, 2015, **19**:497 [Crossref], [Google Scholar], [Publisher]

[71]. Ravindranadh K., Prasad K.D.V., Rao M. Spectroscopic and luminescent properties of Co<sup>2+</sup> doped tin oxide thin films by spray pyrolysis, *AIMS Materials Science*, 2016, **3**:796 [Crossref], [Google Scholar], [Publisher]

[72]. Okorieimoh C., Chime U., Nkele A.C., Nwanya A.C., Madiba I.G., Bashir A., Botha S., Asogwa P.U., Maaza M., Ezema F.I. Room-temperature synthesis and optical properties of nanostructured Ba-Doped ZnO thin films, *Superlattices and Microstructures*, 2019, **130**:321 [Crossref], [Google Scholar], [Publisher]

[73]. Onu C.P., Ekpunobi A.J., Okafor C.E., Ozobialu L.A. Optical properties of monazite nanoparticles prepared via ball milling, *Asian Journal of Research and Reviews in Physics*, 2023, **7**:17 [Crossref], [Google Scholar], [Publisher]

[74]. Jeroh D., Ekpunobi A., Okoli D. Growth of nanostructured zinc selenide films doped with europium and their possible applications, *Applied Nanoscience*, 2023, **13**:4605 [Crossref], [Google Scholar], [Publisher]

- [75]. Muogbo I.P., Ekpunobi A.J., Okoli N.L. Exploring the optical, structural, morphological, and compositional properties of electrosynthesized FeSe/CrSe superlattice thin films, *Journal of Medicinal and Nanomaterials Chemistry*, 2023, **5**:307 [[Crossref](#)], [[Google Scholar](#)], [[Publisher](#)]
- [76]. Awada C., Whyte G.M., Offor P.O., Whyte F.U., Kanoun M.B., Goumri-Said S., Alshoabi A., Ekwealor A.B., Maaaza M., Ezema F.I. Synthesis and studies of electro-deposited yttrium arsenic selenide nanofilms for opto-electronic applications, *Nanomaterials*, 2020, **10**:1557 [[Crossref](#)], [[Google Scholar](#)], [[Publisher](#)]
- [77]. Ganesan K., Anandhan N., Marimuthu T., Panneerselvam R., Roselin A.A. Effect of deposition potential on synthesis, structural, morphological and photoconductivity response of Cu<sub>2</sub>O thin films by electrodeposition technique, *Acta Metallurgica Sinica (English Letters)*, 2019, **32**:1065 [[Crossref](#)], [[Google Scholar](#)], [[Publisher](#)]
- [78]. Kumar K.D.A., Valanarasu S., Ganesh V., Shkir M., AlFaify S., Algarni H. Effect of potential voltages on key functional properties

- of transparent AZO thin films prepared by electrochemical deposition method for optoelectronic applications, *Journal of materials research*, 2018, **33**:1523 [[Crossref](#)], [[Google Scholar](#)], [[Publisher](#)]
- [79]. Salim H., Olusola O., Ojo A., Urasov K., Dergacheva M., Dharmadasa I. Electrodeposition and characterisation of CdS thin films using thiourea precursor for application in solar cells, *Journal of Materials Science: Materials in Electronics*, 2016, **27**:6786 [[Crossref](#)], [[Google Scholar](#)], [[Publisher](#)]

**How to cite this manuscript:** V. C. Onuabuchi, A. Ullah, N. J. Opene, T. Yanlong, C. I. Elekalachi, N. L. Okoli. Effect of deposition potential on the structural and optical properties of electrodeposited antimony doped zinc telluride (Sb:ZnTe) thin films for optoelectronic applications. *Journal of Medicinal and Nanomaterials Chemistry*, 2024, **6**(1), 46-63. DOI: 10.48309/JMNC.2024.1.5